



# Radar measurements of turbulence, electron densities, and absolute reflectivities during polar mesosphere winter echoes (PMWE)

Franz-Josef Lübken \*, Werner Singer, Ralph Latteck, Irina Strelnikova

*Leibniz Institute of Atmosphere Physics, Schloss-Str. 6, 18225, Kühlungsborn, Germany*

Received 10 October 2006; received in revised form 5 January 2007; accepted 8 January 2007

## Abstract

On January 21, 2005, strong radar echoes known as ‘polar mesosphere winter echoes’ (PMWE) were observed by the ALWIN VHF radar at 69°N. Peak reflectivities of  $\sim 10^{-14}/\text{m}$  were observed at approximately 13 UT. At the same time the Saura MF radar which is only  $\sim 15$  km away from ALWIN measured electron densities ( $N_e$ ) and turbulence energy dissipation rates ( $\epsilon$ ). This combination is rather seldom because PMWE are rare (occurrence rate is 1–2%) and electron densities are critical: too low values do not give a PMWE, and too large values prohibit to derive  $N_e$  due to signal absorption. At PMWE altitudes ( $\sim 62$  km) typical energy dissipation rates before, during, and after the PMWE are  $\epsilon \sim 100$  mW/kg. The electron density during the PMWE is typically  $10^9/\text{m}^3$  and much smaller prior to PMWE. We have applied a theoretical model based on turbulence theory to derive absolute reflectivities for these  $\epsilon$  and  $N_e$  values and arrive at  $\sim 2 \times 10^{-15}/\text{m}$  during PMWE (in nice agreement with measurements) and  $\sim 3 \times 10^{-17}/\text{m}$  outside PMWE. The latter value is indeed below the detection limit of the ALWIN radar. The nice quantitative agreement between measured and calculated absolute volume reflectivities confirms earlier conclusions that neutral air turbulence is the main cause for PMWE. Furthermore, we have analyzed the autocorrelation function of the EISCAT 224 MHz PMWE observations from November 10, 2004, and find that the spectral form is different inside the PMWE compared to outside. The shape is Gaussian inside PMWE (compatible with turbulent scatter), whereas it is Lorentzian above the PMWE, indicating non-turbulent, incoherent scatter.

© 2007 COSPAR. Published by Elsevier Ltd. All rights reserved.

*Keywords:* Winter polar mesosphere; Radar echoes; Turbulence; Polar mesosphere; Winter echoes; VHF radar

## 1. Introduction

Radars are widely used to deduce atmospheric quantities analyzing characteristics of backscattered signal such as strength and spectral width. It is therefore essential to understand the underlying physical process leading to the backscatter before any atmospheric parameter can be derived. Since several years peculiar radar echoes are observed in the lower winter mesosphere at mid and high latitudes, called ‘polar mesosphere winter echoes’ (PMWE). VHF radar observations in the winter mesosphere have been observed since many years at mid and high latitudes (see, for example, Ecklund and Balsley, 1981; Röttger et al., 1979). More recent results regarding

PMWE are presented in the literature (e.g. Kirkwood et al., 2006a; Lübken et al., 2006; Zeller et al., 2006; Brattli et al., 2006). A similar phenomenon is known from the summer mesopause region at middle and polar latitudes and is called ‘(polar) mesosphere summer echoes’, (P)MSE. It is known since several years that (P)MSE are strongly related to charged ice particles which reduce the diffusivity of free electrons leading to Schmidt numbers  $Sc$  much larger than unity ( $Sc = \nu/D$ ;  $D$  = diffusivity of electrons;  $\nu$  = kinematic viscosity). The low electron diffusivity allows fluctuations at the radar Bragg scale ( $\lambda/2 = 3$  m for a 50 MHz VHF radar) which would otherwise be destroyed by molecular diffusion (see recent review by Rapp and Lübken, 2004, for more details). A similar process was suggested for PMWE although there is no direct evidence for ‘large’ aerosol particles in the lower winter mesosphere. PMWE typically occur in the lower

\* Corresponding author. Tel.: +49 38293 680; fax: +49 38293 6850.  
E-mail address: [luebken@iap-kborn.de](mailto:luebken@iap-kborn.de) (F.-J. Lübken).

mesosphere where the kinematic viscosity  $\nu$  is orders of magnitude larger compared to the summer mesopause region. This allows the existence of small scale structures (e.g. at  $\lambda/2 = 3$  m) in the neutral and charged atmosphere caused by neutral air turbulence, even if  $Sc = 1$ .

Whether or not turbulence is causing PMWE can best be tested by measuring turbulent parameters during a PMWE event. Unfortunately, PMWE are difficult to study experimentally since they occur much more seldom than PMSE (typical occurrence frequencies at polar latitudes are 1–2% and 80–100%, respectively; see Zeller et al., 2006). In January 2005 a field campaign took place at the Andøya Rocket Range (69°N) comprising radar observations and launchings of 23 sounding rockets. Serendipitously, several strong PMWE developed during the campaign due to strong solar and/or geomagnetic activity which led to strong ionization in the D-region. An overview about of the campaign and first results have recently been published (Lübken et al., 2006; Brattli et al., 2006). The in situ and ground based measurements give strong evidence that turbulence in combination with large electron densities has indeed caused PMWE. The positive ion probe instrument (PIP) on board of sounding rockets showed turbulence like spectra at PMWE heights. Energy dissipation rates  $\epsilon$  are frequently derived from turbulence spectra (more precisely from the ‘inner scale’,  $\ell_o^H$ ) following the procedure introduced by Lübken (1992). Unfortunately, this procedure cannot be applied to the PIP data since  $\ell_o^H$  is only a few meters in the lower mesosphere. The power spectral density from turbulence at these scales is very small and is embedded in the instrumental noise of PIP. However, turbulence parameters are deduced from the spectral width measurements performed by the Saura MF radar which is located only a few kilometers away from the VHF radar and from the rocket range. This radar also gives electron densities which are important to deduce the absolute volume reflectivity inside PMWE (see below). In this paper we report on first simultaneous and co-located measurements of PMWE, electron density, and turbulence by various radars installed close to the Andøya Rocket Range (69°N).

## 2. Instrumentation and observations

### 2.1. PMWE measurements by VHF radar

Coherent radar backscatter at 53.5 MHz above 50 km have been observed with the ALWIN MST radar located close to the Andøya Rocket Range. The radar is calibrated which allows to derive absolute echo power from the vertical beam in the altitude range 50–114 km with 300 m range resolution applying a 16-bit complementary code. Finally, absolute volume reflectivity is deduced (Latteck, 2005b) which can directly be compared with other calibrated radars and with model results on coherent radar backscatter in weakly ionized media. PMWE were observed during a period of strongly enhanced solar activity and geomag-

netic activity between January 17 and 21, 2005. The strongest event appeared on January 20 related to a severe solar proton event (see also Lübken et al., 2006). This PMWE extended over a height range between 53 and 78 km for about 8 h centered around local noon. The excessive ionization due to high energetic particles prevented the MF radar to measure electron densities (see below). In this paper we therefore concentrate on a weaker PMWE from January 21 when the ionization was decaying and simultaneous observations of the height region below about 75 km were performed by the VHF radar and the Saura MF radar. In Fig. 1 we show the polar mesosphere winter echoes observed with the ALWIN MST radar on January 21, 2005, when the fluxes of energetic protons were in general decaying but still enhanced. Simultaneous observations of the height region below about 75 km were performed by the VHF radar and the Saura MF radar. The electron density enhancement around noon on January 21 goes along with two M-class X-ray flares in the 1–8 Å band and increasing proton fluxes with energies less than 10 MeV which are probably related to trapped outer-zone particles. The geomagnetic activity was slightly enhanced ( $K_p = 3$  at Tromsø). Strong echoes appear around 62 km with volume reflectivities up to  $\sim 10^{-14}$ /m. The echoes last for approximately 2.5 h. Some sporadic minor echoes are observed at higher altitudes. We cannot make a quantitative analysis for these echoes since no electron density nor energy dissipation rate data are available at these heights because the Saura signal is too weak.

### 2.2. Turbulence measurements by MF radar

The Saura MF radar is located about 15 km southward of the Andøya Rocket Range and is operated at 3.17 MHz with a peak power of 116 kW (Singer, 2006). The narrow beam transmitting/receiving antenna consists of 29 crossed

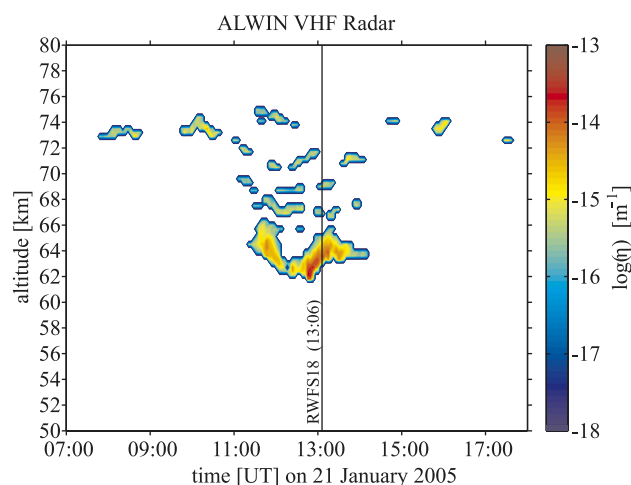


Fig. 1. Radar reflectivities (1/m) measured by the ALWIN VHF radar at 69°N on 21 January 2005. A falling sphere labeled ‘RWFS18’ was launched at 13:06 UT, i.e., around the maximum of the PMWE.

half-wave dipoles arranged as a Mills Cross resulting in a beam width of only  $6.4^\circ$  (full width at half power). Antenna and transceiver system provide high flexibility in beam forming and pointing as well as the capability forming beams with right and left circular polarization (ordinary and extraordinary magneto-ionic component). The narrow beam is essential for reliable turbulence measurements using spectral widths since non-turbulence broadening caused by background winds ('beam broadening', 'shear broadening') are small and can be corrected using winds measured by the same radar at the same time (Hocking, 1983; Latteck et al., 2005a). Hourly means of turbulent energy dissipation rates are derived from the corrected spectral width and the Brunt-Väisälä frequency taken from in situ falling sphere measurements or from a climatology (Lübken, 1999). The Saura MF radar continuously provides horizontal winds, turbulence parameters, and electron densities in a 9 min sequence of tilted and vertically directed beams in height steps of 1 km. Interleaved transmission of ordinary and extraordinary polarization allows differential absorption (DAE) and differential phase (DPE) measurements. Electron density profiles are derived from the DAE and DPE experiments separately and are combined to a mean profile provided that the DAE and DPE results do not differ by more than a factor of two (Singer, 2005). The electron density profiles cover an altitude range of 60–85 km under undisturbed ionospheric conditions and reach down to 55 km under disturbed conditions (geomagnetic disturbances and/or solar activity storms). The height coverage of the MF radar is sometimes reduced by enhanced background noise due to external interference or by excessively large ionization which strongly attenuates the extraordinary component. This happened on January 18 and 20, 2005, and prevented reliable electron density measurements within PMWE on these days.

In Fig. 2 we show turbulent energy dissipation rates  $\epsilon$  measured before, during, and after the PMWE event on January 21. The  $\epsilon$  values are of comparable strength indicating that turbulence is persistent for several hours at altitudes below about 75 km. During the PMWE event the energy dissipation rates vary in the range 50–160 mW/kg caused by natural variability which is somewhat larger compared to the climatology from rocket measurements presented in Lübken (1997). There is no obvious geophysical reason for this enlarged turbulence activity. We note that the temperature profile measured by falling sphere flight RWFS18 shows reduced static stability in the 55–65 km height range which is presumably caused by persistent and strong turbulent mixing (see Fig. 3 in Lübken et al., 2006). Furthermore, part of this difference may be due to the uncertainties in the absolute radar values which, however, does not significantly affect our conclusions since the PMWE strength is fairly insensitive to  $\epsilon$ . Simultaneously performed electron density observations before and during the PMWE event (Fig. 3) show an increase of electron density by about one order of magnitude during the PMWE event and at PMWE altitudes. During the PMWE

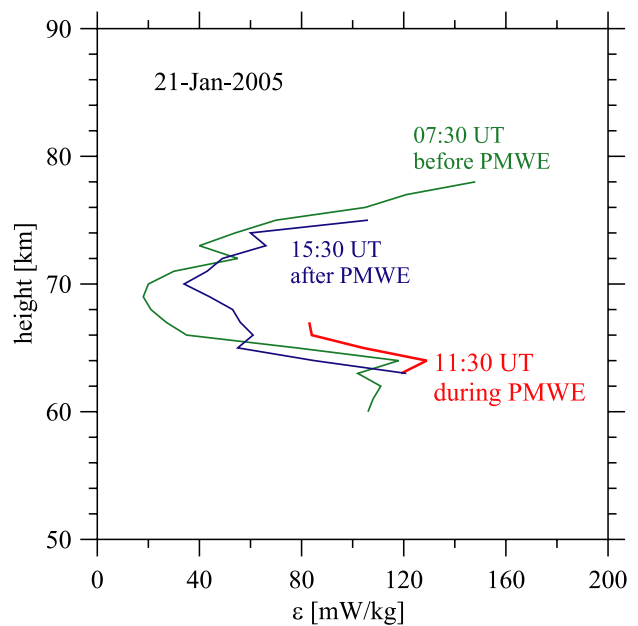


Fig. 2. Turbulent energy dissipation rates measured by the Saura MF radar on 21 January 2005. Different colors present different times before (green), during (red), and after (blue) the PMWE, respectively. (For interpretation of the references in colour in this figure legend, the reader is referred to the web version of this article.)

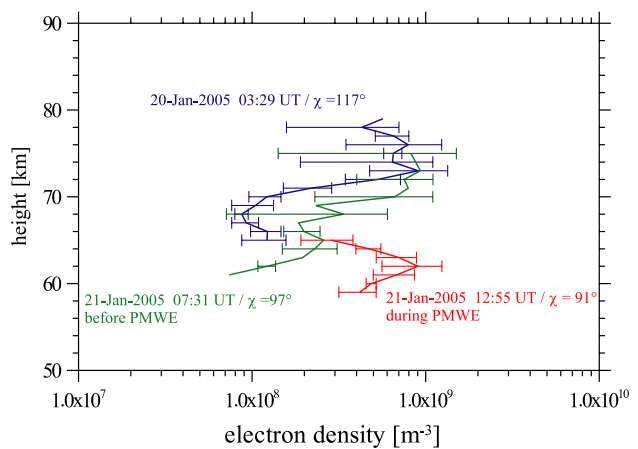


Fig. 3. Electron density profiles measured by the Saura MF radar on 21 January 2005. MF radar results are shown at a few hours before (green), during (red), and one day before (blue) the PMWE at solar zenith angles ( $\chi$ ) between  $91^\circ$  and  $117^\circ$ . The horizontal bars indicate natural variability. (For interpretation of the references in colour in this figure legend, the reader is referred to the web version of this article.)

(more precisely from 12:47 UT to 13:14 UT) the peak electron densities are  $N_e = 9 \times 10^8 \pm 3.6 \times 10^8 \text{ m}^{-3}$ .

A similar set of simultaneous observations of absolute radar reflectivity, turbulent energy dissipation rate, and electron density is also available from January 19 again during (weak) PMWE between about 11:00 and 15:00 UT. As in the case discussed in more detail below we find good agreement between measured reflectivities and theoretical expectations based on turbulence theory and measurements of  $N_e$  and  $\epsilon$ .

### 3. Discussion and interpretation

The theory of coherent radar backscatter from a weakly ionized plasma is summarized in the literature (Tatarskii, 1961; Hill, 1979). The application to turbulent PMSE and PMWE yields the absolute volume reflectivity  $\eta$  as a function of wavenumber, turbulent energy dissipation rate  $\epsilon$ , dissipation rate of fluctuations  $N_{\vartheta}$ , Schmidt number  $Sc$ , and mean electron density  $\bar{N}_e$  (see Lübken et al., 2006, for more details). In Fig. 4 we show theoretically expected radar reflectivities as function of  $\bar{N}_e$  and  $\epsilon$  using  $\nu = 0.091 \text{ m}^2/\text{s}$  (representative for 62 km),  $Sc = 1$ , and  $N_{\vartheta} = 1 \times 10^{-5}/\text{s}$ . The latter value is taken from rocket measurements of neutral air density fluctuations and considerations about the mean gradient of electron versus neutral air density (Lübken et al., 2006). For  $\epsilon \sim 0,1 \text{ W/kg}$  and mean electron densities of  $10^8/\text{m}^3$  and  $10^9/\text{m}^3$  we find typical reflectivities of  $10^{-17}/\text{m}$  and  $10^{-15}/\text{m}$ , respectively. In Fig. 5 we compare these theoretical values with measurements prior to and during PMWE. As can be seen from this plot, the theoretical expectation nicely matches the observations, i.e. the measured  $\eta$  value during PMWE is in agreement with theory, and  $\eta$  outside PMWE is too small to be detected by the radar. This nicely confirms the idea that neutral turbulence has caused PMWE, in addition to the arguments already discussed in Lübken et al. (2006) and Brattli et al. (2006). We consider the remaining difference between prediction and measurements by a factor of  $\sim 6$  not problematic taking into account the uncertainties in the absolute radar measurements and the parameters and geophysical values used in the prediction.

An alternative approach to calculate absolute reflectivities is based of estimates of the structure function constant

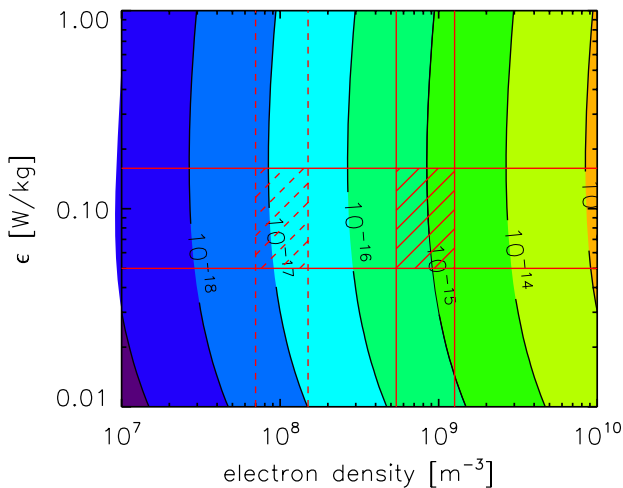


Fig. 4. Theoretical values of the absolute radar reflectivity  $\eta$  in  $1/\text{m}$  as a function of electron densities and energy dissipation rates using a kinematic viscosity of  $\nu = 0.091 \text{ m}^2/\text{s}$  representative for an altitude of 62 km. We have used  $Sc = 1$  and  $N_{\vartheta} = 1 \times 10^{-5}/\text{s}$  in this plot (see text for more details). The red lines indicate measured values (including natural variability and uncertainties; see text) of energy dissipation rates and electron densities during (solid lines) and prior to (dashed lines) the PMWE measured on January 21, 2005.

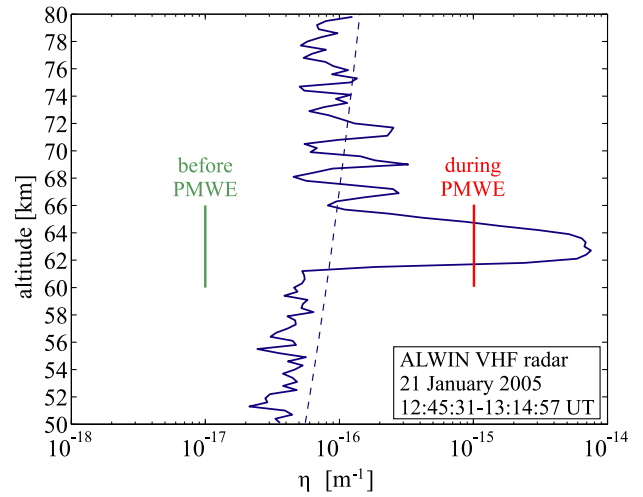


Fig. 5. Absolute radar reflectivity measured by the ALWIN VHF radar on 21 January 2005 in the period 12:45–13:14 UT, i.e. during the rocket launch of a falling sphere labeled ‘RWFS18’ (see Fig. 1). The red and green bar indicate the theoretical calculation of  $\eta$  using electron densities and energy dissipation rates during (red) and before (green) the PMWE. The dashed line represents the reflectivity detection limit of the radar which is also used as the cut-off value in Fig. 1. (For interpretation of the references in colour in this figure legend, the reader is referred to the web version of this article.)

and the variation of the refractive index with electron density (Hocking, 1985). This formalism is sometimes used in the literature to estimate  $\eta$  from  $\bar{N}_e$  and the mean electron density gradient  $d\bar{N}_e/dz$  (Stebel et al., 2004). In Fig. 6 we show theoretical values for  $\eta$  as a function of  $\bar{N}_e$  and  $-H_e$  ( $H_e$  is the scale height of electron density which is

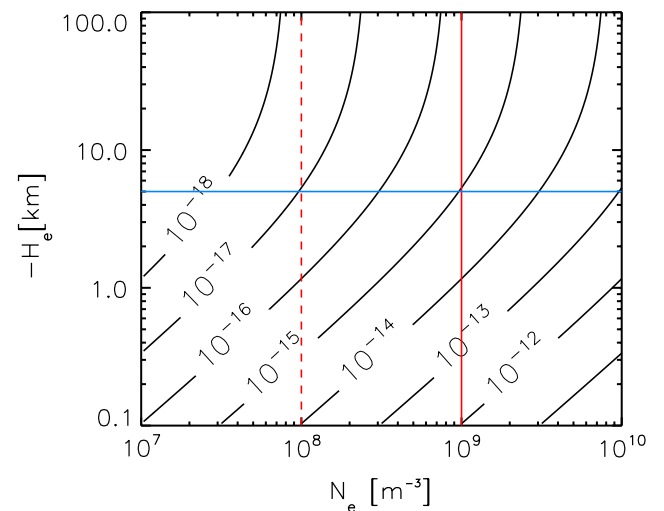


Fig. 6. Theoretical values of absolute radar reflectivity  $\eta$  in  $1/\text{m}$  as a function of electron densities and electron density scale height. We have used a kinematic viscosity of  $\nu = 0.091 \text{ m}^2/\text{s}$  (representative for  $z = 62 \text{ km}$ ),  $Sc = 1$ , and  $\epsilon = 0.1 \text{ W/kg}$  in this plot (see text for more details). The red lines indicate electron densities measured during (solid line) and prior (dashed line) to the PMWE measured on January 21, 2005. An electron density scale height of  $H_e = -5 \text{ km}$  is indicated (blue line) as typical for the D-region. (For interpretation of the references in colour in this figure legend, the reader is referred to the web version of this article.)

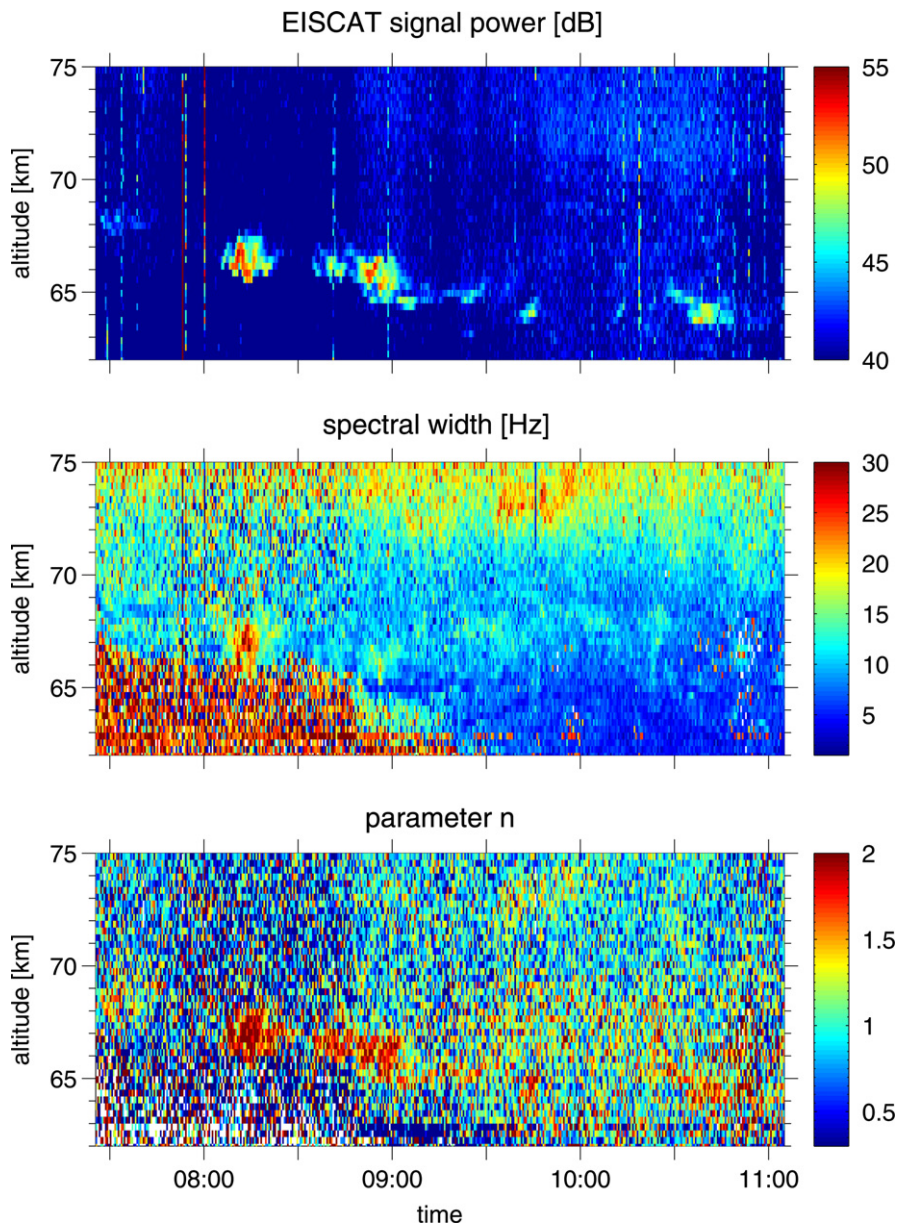


Fig. 7. EISCAT 224 MHz radar results from November 10, 2004, during a solar proton event. Top panel, signal power; mid panel, spectral width; lower panel, parameter  $n$  describing the shape of the spectrum (see text).

negative in the D-region since  $\overline{N_e}$  increases with altitude). A typical value is  $-H_e = 1\text{--}10$  km. We note that the electron density scale height changes sign within the PMWE layer. We have not considered these variations in detail but taken a typical value instead, because of the uncertainties introduced by the experimental method and the horizontal distance between the radar and rocket measurements. In Fig. 6 we have used background conditions typical for 62 km and the energy dissipation rate of 0.1 W/kg measured by the MF radar (see above). As can be seen from this figure a scale height of  $-H_e = 5$  km (see Fig. 3) and mean electron densities of  $10^8/\text{m}^3$  and  $10^9/\text{m}^3$  lead to typical reflectivities of  $10^{-17}/\text{m}$  and  $10^{-15}/\text{m}$ , respectively, in nice agreement with our calculations presented above. This agreement is in fact surprising since various assumptions

are used to derive  $\eta(\overline{N_e}, d\overline{N_e}/dz, \dots)$ , for example a certain Richardson number (we use  $Ri = 1$ , as in Stebel et al., 2004). We take this agreement as a nice confirmation that our calculations of  $\eta$  using  $\overline{N_e}$ ,  $d\overline{N_e}/dz$ , and  $N_D$  indeed give reliable estimates of the absolute reflectivities.

The nice quantitative agreement between measured and calculated absolute radar reflectivities confirms our earlier conclusion that neutral air turbulence has caused PMWE. We have used  $Sc = 1$  in all our calculations, i.e. an enhanced Schmidt number is obviously of minor importance for PMWE. This is in contrast to PMSE in the upper mesosphere which requires large  $Sc$  values. The different sensitivity of radar echoes (PMWE versus PMSE) on turbulence can be understood by considering the rapid increase of kinematic viscosity with height. Turbulence

energy dissipation rates required to make  $\ell_o^H = 3\text{m}$  are proportional to  $1/\rho^3$ . To fulfill this condition turbulence has to increase by six orders of magnitude (!) from 55 to 85 km. Our results also confirm the importance of sufficiently large electron densities and turbulence to get PMWE. The VHF radar detects PMWE when the electron density reaches a level that existing turbulence generates fluctuations in the plasma at the radar Bragg scale which are strong enough to cause observable radar backscatter. This explains why PMWE occurs only during disturbed solar and/or geomagnetic conditions, i.e., when ionization is large in the D-region.

In a recent paper Kirkwood et al. (2006b) study the EISCAT 224 MHz echoes during PMWE on 10 November 2004 when a solar proton event was present. They argue that turbulence cannot have caused the echoes since the spectral width is similar inside the PMWE layer compared to above and below. This brings them to speculate that the echoes might have been caused by highly damped viscosity waves which are generated when gravity waves or infrasound waves are partially reflected at a horizontally stretched inhomogeneity in temperature or wind. We will not discuss this suggestion here but want to present our results regarding the spectral form of the EISCAT echoes. In Fig. 7 we show results from the case discussed by Kirkwood et al. (2006b), namely the echo power, the spectral widths, and a parameter  $n$  which is defined as follows. Following Jackel (2000) the autocorrelation function (ACF) is a complex function which can be written in terms of magnitude and phase:  $\text{ACF}(t) = \text{ACF}(t_0) \cdot e^{-(\pi W t)^n} \cdot e^{i\phi(t)}$ , where  $t$  is time,  $W$  is the spectral width and  $\phi$  is the phase. The shape of the ACF magnitude is controlled by the parameter  $n$ :  $n = 1$  represents a Lorentzian spectral shape as expected for incoherent scatter and  $n = 2$  represents a Gaussian shape expected for turbulent scatter. As can be seen from Fig. 7 the parameter  $n$  is close to 2 in the entire PMWE layer indicating that turbulence has caused the echoes, whereas it is significantly closer to 1 outside, indicating incoherent scatter (as expected). We do not yet know whether  $n = 2$  excludes the infrasound process suggested by Kirkwood et al. (2006b) since the spectral form of this complicated mechanism is not yet known. We note that sometimes the spectral width is indeed different within the PMWE layer compared to above (see, e.g., around 8:15 UT in Fig. 7). There are other times when the difference is negligible. Since for fixed  $\lambda$  the spectral width is proportional to  $\sqrt{\epsilon/\omega_B}$  ( $\omega_B =$  Brunt-Väisälä frequency) we speculate that the periods of rather low widths come from low turbulence and/or from high  $\omega_B$  values.

Simultaneous measurements of PMWE,  $N_e$ , and  $\epsilon$  are seldom because (i) PMWE are very rare and (ii) the electron density is critical: too low values do not give a PMWE, and too large values prohibits to derive  $N_e$  (see above). In summary, we have shown that radar measurements of electron densities and turbulent energy dissipation rates lead to theoretically derived volume reflectivities which agree quantitatively with the radar observations during PMWE.

Outside PMWE the same combination of measurements results in approximately two orders of magnitude smaller reflectivities, again in agreement with the non-existence of PMWE. This nice quantitative agreement between measured and expected reflectivities (from turbulence theory) further supports the idea that neutral turbulence is the prime mechanism creating PMWE.

### Acknowledgements

We thank Dr. Markus Rapp for helpful discussions. The project is partly funded by the Bundesministerium für Bildung, Wissenschaft, Forschung und Technologie, Bonn, under grant 50 OE 99 01 (ROMA), and by the Deutsche Forschungsgemeinschaft under the CAWSES SPP grant LU 1174/3-1 (SOLEIL). EISCAT is an international scientific association supported by the research councils of Finland (SA), France (CNRS), Germany (MPG), Japan (NIPR), Norway (RCN), Sweden (NFR) and the United Kingdom (PPARC). The radar experiments received funding from the EU 6th framework programme project ALOMAR EARI.

### References

- Brattli, A., Blix, T.A., Lie-Svendsen, Ø, Hoppe, U.-P., Lübken, F.-J., Rapp, M., Singer, W., Latteck, R., Friedrich, M. Rocket measurements of positive ions during polar mesosphere winter echo conditions. *Atmos. Chem. Phys.* 6, 5515–5524, 2006.
- Ecklund, W.L., Balsley, B.B. Long-term observations of the Arctic mesosphere with the MST radar at Poker Flat, Alaska. *J. Geophys. Res.* 86, 7775–7780, 1981.
- Hill, R.J. Spectra of fluctuations in refractivity, temperature, humidity, and the temperature–humidity cospectrum in the inertial and dissipation ranges. *Radio Sci.* 13, 953–961, 1979.
- Hocking, W.K. On the extraction of atmospheric turbulence parameters from radar backscatter Doppler spectra – i. Theory. *J. Atmos. Terr. Phys.* 45, 89–102, 1983.
- Hocking, W.K. Measurement of turbulent energy dissipation rates in the middle atmosphere by radar techniques: a review. *Radio Sci.* 20, 1403–1422, 1985.
- Jackel, B.J. Characterization of auroral radar power spectra and autocorrelation function. *Radio Sci.* 35, 1009–1023, 2000.
- Kirkwood, S., Belova, E., Blum, U., Croskey, C., Dalin, P., Fricke, K.-H., Goldberg, R.A., Mitchell, J.D., Schmidlin, F. Polar mesosphere winter echoes during MaCWAVE. *Ann. Geophys.* 24, 1245–1255, 2006a.
- Kirkwood, S., Chilson, P., Belova, E., Dalin, P., Häggström, I., Rietveld, M., Singer, W. Infrasound – the cause of strong Polar Mesosphere Winter Echoes? *Ann. Geophys.* 24, 475–491, 2006b.
- Latteck, R., Singer, W., Hocking, W.K. Measurement of turbulent kinetic energy dissipation rates in the mesosphere by a 3 MHz Doppler radar. *Adv. Space Res.* 35 (11), 1905–1910, 2005a.
- Latteck, R., Singer, W., Kirkwood, S., Jönsson, L.O., Eriksson, H. Observation of mesosphere summer echoes with calibrated VHF radars at latitudes between 54°N and 69°N in summer 2004. In: *Proceedings of the 17th ESA Symposium on European Rocket and Balloon Programmes and Related Research*, vol. ESA SP-590. Sandefjord, Norway, pp. 121–126, 2005b.
- Lübken, F.-J. On the extraction of turbulent parameters from atmospheric density fluctuations. *J. Geophys. Res.* 97, 20,385–20,395, 1992.
- Lübken, F.-J. Seasonal variation of turbulent energy dissipation rates at high latitudes as determined by in situ measurements of neutral density fluctuations. *J. Geophys. Res.* 104, 13,441–13,456, 1997.

- Lübken, F.-J. Thermal structure of the Arctic summer mesosphere. *J. Geophys. Res.* 104, 9135–9149, 1999.
- Lübken, F.-J., Strelnikov, B., Rapp, M., Singer, W., Latteck, R., Brattli, A., Hoppe, U.-P., Friedrich, M. The thermal and dynamical state of the atmosphere during polar mesosphere winter echoes. *Atmos. Chem. Phys.* 6, 13–24, 2006.
- Rapp, M., Lübken, F.-J. Polar mesosphere summer echoes (PMSE): review of observations and current understanding. *Atmos. Chem. Phys.* 4, 2601–2633, 2004.
- Röttger, J., Rastogi, P.K., Woodman, R.F. High-resolution VHF radar observations of turbulence structures in the mesosphere. *Geophys. Res. Lett.* 6, 617–620, 1979.
- Singer, W., Latteck, R., Friedrich, M., Dalin, P., Kirkwood, S., Engler, N., Holdsworth, D. D-region electron densities obtained by differential absorption and phase measurements with a 3-MHz doppler radar, In: Proceedings of the 17th ESA Symposium on European Rocket and Balloon Programmes and Related Research, vol. ESA SP-590. Sandefjord, Norway, pp. 233–238, 2005.
- Singer, W., Latteck, R., Holdsworth, D.A. A new narrow beam Doppler radar at 3 MHz for studies of the high-latitude middle atmosphere, *Adv. Space Res.* Submitted for publication.
- Stebel, K., Blum, U., Fricke, K.-H., Kirkwood, S., Mitchell, N.J., Osepian, A. Joint radar/lidar observations of possible aerosol layers in the winter mesosphere. *J. Atmos. Solar Terr. Phys.* 66, 957–970, 2004.
- Tatarskii, V.I. *Wave Propagation in a Turbulent Medium*. McGraw-Hill Book Comp., New York, 1961.
- Zeller, O., Zecha, M., Bremer, J., Latteck, R., Singer, W. Mean characteristics of mesosphere winter echoes at mid- and high-latitudes. *J. Atmos. Solar Terr. Phys.* 68, 1087–1104, 2006.